DMD Fast Forward. Published on October 17, 2024 as DOI: 10.1124/dmd.124.001817
This article has not been copyedited and formatted. The final version may differ from this version.

Intestine vs. Liver？Uncovering the Hidden major Metabolic organs of Silybin in Rats

Yuanbo Sun[a, b, 1], Like Xie [a, b, 1], Jing Zhang [a, b, 1], Runing Liu [a, b], Hanbing Li [a, b], Yanquan Yang [a, b], Yapeng Wu [a, b], Ying Peng [a, b], Guangji Wang [a, b], Natalie Medlicott [c], Jianguo Sun [a, b *]

[a] *Jiangsu Provincial Key Laboratory of Drug Metabolism and Pharmacokinetics, Research Unit of PK-PD Based Bioactive Components and Pharmacodynamic Target Discovery of Natural Medicine of Chinese Academy of Medical Sciences, China Pharmaceutical University, Nanjing, 210009, China*

[b] *State Key Laboratory of Natural Medicines, China Pharmaceutical University, Nanjing, 210009, China*

[c] *School of Pharmacy, University of Otago, Dunedin, New Zealand*

[1] *Yuanbo Sun, Like Xie and Jing Zhang contributed equally to this work and share first authorship.*

Running Title: Determination of main metabolic organs of silybin in rats

***Corresponding author**

Prof. Jianguo Sun,

a, Jiangsu Provincial Key Laboratory of Drug Metabolism and Pharmacokinetics, Research Unit of PK-PD Based Bioactive Components and Pharmacodynamic Target Discovery of Natural Medicine of Chinese Academy of Medical Sciences, China Pharmaceutical University Nanjing, 210009, China

b, State Key Laboratory of Natural Medicines, China Pharmaceutical University, Nanjing, 210009, China

Tel: 025-83271176

E-mail: jgsun@cpu.edu.cn

Text pages 19

Table count 2

Figure count 5

Reference count 20

Abstract 171words

Introduction 446 words

Discussion 984 words

DMD Fast Forward. Published on October 17, 2024 as DOI: 10.1124/dmd.124.001817
This article has not been copyedited and formatted. The final version may differ from this version.

Abbreviations:

Q-TOF, Quadrupole-Time of Flight; NAR, Naringin; HPLC, High Performance Liquid Chromatography; ESI, Electrospray Ionisation Source; XIC, Extracted Ion Chromatogram; IS, Internal Standard; IDA, information-dependent acquisition; PK, Pharmacokinetics; AUC, Area Under Curve; ER, Extraction Ratio; $t_{1/2\beta}$, half life time; T_{max}, peak time; C_{max}, peak concentration; SD, standard deviation.

Significance Statement.

This study confirmed the main metabolism place of silybin in rats were gastrointestinal tracts instead of livers and the intestinal microbes were closely involved. Then 29 (out of 32) metabolism pathways and 56 (out of 59) metabolites were identified for the first time in rats. And to further study the liver disposition of silybin, its hepatic first-pass effect was determined for the first time.

DMD Fast Forward. Published on October 17, 2024 as DOI: 10.1124/dmd.124.001817
This article has not been copyedited and formatted. The final version may differ from this version.

Abstract

Silybin, extracted milk thistle, was a flavonolignan compound with hepatoprotective effect. Now it is commonly used in dietary supplements, functional foods, and nutraceuticals. However, the metabolism of silybin has not been systematically characterized in organisms to date. Therefore, we established a novel HPLC-Q-TOF/MS method to analyze and identify the prototype and metabolites of silybin in rats. Totally, 29 (out of 32) new metabolic pathways and 56 (out of 59) unreported metabolite products were detected. Moreover, we found that the liver had a high first-pass effect of 63.30%±13.01 for silybin and only one metabolite was detected. And the metabolites identified in gastrointestinal tract possessed 88% of all (52 out of 59). At the same time, the high concentration of silybin in the livers also indicated large amounts of silybin may be accumulated in liver instead of being metabolized. These results indicated the primary metabolizing organ of silybin in rats was intestine rather than liver, which would also offer solid chemical foundation for exploring more promising health care products of silybin.

Keywords: Silybin, HPLC-MS/MS, Metabolism, Hepatic first-pass effect, Pharmacokinetics

1.Introduction

Silybin is a natural compound extracted from the seeds of the milk thistle plant in the asteraceae family, which is also the main active ingredient of milk thistle (Tuli et al., 2021). It has long been widely used in Asia and Europe for the clinical treatment of liver diseases (Bijak, 2017). In addition, in several clinical trials of patients with non-alcoholic fatty liver disease and patients with non-cirrhotic chronic hepatitis C, many of the key factors improved faster and better in patients taking silybin compared to those taking placebo (Abenavoli et al., 2015; Wah Kheong et al., 2017). Modern pharmacological studies have also demonstrated its antioxidant (Tvrdý et al., 2021), anticancer (Yassin et al., 2022) and other pharmacological functions. And the number of relevant studies is increasing every year which can be reflected in the large number of papers published in recent years (more than 100 papers per year on average between 2013 and 2022 (PubMed)).

In addition, many studies have focused on the positive effects of silybin on liver disease, as well as other diseases, by mediating the intestinal flora through the gut-liver axis. (Xu et al., 2018; Shen et al., 2019). And it is well known that the basis for the pharmacological effect is laid mainly by the compound itself and its metabolites. However, there is no complete assessment of the metabolic pathway of silybin in *vivo*. In *vivo* studies now have focused on its biotransformation in human and animal feces and urine, including a series of phase II metabolites: sulfate, monoglucuronide, diglucuronide, and triglucuronide metabolites, as well as the glucuronide metabolites of O-methyl silybin and silybin sulfate (Hoh et al., 2007; Marhol et al., 2015; Bai et al., 2021; Xu et al., 2022). In in *vitro* studies, glutathione, glucuronidation, demethylation, and other metabolic reactions were detected in the fungus (Abourashed et al., 2012), gut bacteria (Zhang et al., 2014), liver microsomes between species (Gunaratna and Zhang,

DMD Fast Forward. Published on October 17, 2024 as DOI: 10.1124/dmd.124.001817
This article has not been copyedited and formatted. The final version may differ from this version.

2003), human hepatocyte (Pferschy-Wenzig et al., 2023). Such metabolic studies are not sufficient to explain the rich and excellent pharmacological activity of silybin. Therefore, in the present study, we have evaluated the comprehensive metabolic pathways and unnoticed metabolic organs of silybin in rats after oral administration for the first time.

Additionally, considering that silybin as an excellent hepatoprotective drug, the liver supposed to be the main metabolizing organ of silybin and its disposition to silybin deserves further investigation, the present study further determined the liver distribution of silybin including hepatic first-pass effect and the concentration in the liver based on the metabolic pathway of silybin in *vivo* in rats. In conclusion, these works will provide a solid chemical basis for the study of the biological characterization of silybin.

2 Experimental Procedures

2.1 Reagents and Chemicals

Silybin was purchased from Medbio Pharmaceutical Technology Company, (purity＞95%; Shanghai, China). Acetonitrile and methanol of HPLC-grade we supplied by Merck (Darmstadt, Germany). HPLC-grade formic acid and Sodium carboxymethyl cellulose (CMC-Na) and HPLC-grade formic acid were provided from Sigma-Aldrich Chemicals (St. Louis, MO). HPLC-grade ultrapure water was filtered from the Milli-Q system. Other reagents and materials were of commercial analytical purity.

2.2 Animals Studies

Metabolism study and Pharmacokinetics study: Male Sprague−Dawley (SD) rats (200±20 g) were purchased from Vital River Laboratory Animal Technology Co., Ltd. (Beijing, China). All the animals were raised under the standard humidity, temperature and light for a week with free food and water for a week. Then the rats were fasted overnight with unlimited water before experiments. All the animal studies

were conducted according to the procedures approved (CPU-PK-202205-008) by the Animal Ethics Committee of China Pharmaceutical University (Nanjing, China).

2.2.1 Metabolism Study

Thirty-nine SD rats (male) were classified into A, B, C and D group (30, 3, 3, 3 each). Initially, silybin was suspended in 0.5% CMC-Na, then group ABC were given the drug orally with the dosage of 200 mg/kg. Moreover, group D received 0.5% CMC-Na with equal dosage as the blank group. 5% Chloral hydrate was used to anesthetize rats in A group at 10 min, 20 min, 30 min, 45 min, 1 h, 2 h, 3 h, 4 h, 6 h, 12 h (n=3) after silybin. Then the blood from hepatic vein was acquired firstly and abdominal aorta plasma was collected to sacrifice. The anticoagulant used in plasma collection was 1% sodium heparin solution. Simultaneously, hearts, livers, spleens, lungs, kidneys, stomachs, ileal, cecum, colon, gastric contents, ileal contents, cecal contents, colon contents were acquired. Plasma samples were obtained from blood by centrifuging at 4 ℃ 8000 rpm, 5 min. Rats in B group were housed in metabolism cages to collect urine and feces. Firstly, the blank samples were acquired before administration, and then after silybin administration, samples were collected within 24 h. 5% urethane was used to anesthetize rats in C group (n=3), then the rats received the bile duct cannulation surgery. The bile samples were obtained during 0-12 h. Rats in D group were administered with 0.5% CMC-Na with the same treatment as the corresponding groups. All the samples were kept at -80 ℃ until analysis.

2.2.2 Pharmacokinetics Study

In accordance with the conventional methods, 40 SD male rats were classified into 8 groups randomly. The rats were given silybin (dissolved in ethanol-PEG200 (1:1) solution based on the previous study by oral administration with dosage of 200 mg/kg. 5%. urethane was injected by abdominal cavity for

DMD Fast Forward. Published on October 17, 2024 as DOI: 10.1124/dmd.124.001817
This article has not been copyedited and formatted. The final version may differ from this version.

anesthesia after 0.17, 0.33, 1, 2, 4, 8, 12h. (n=5), after administration. The blood of hepatic portal vein was collected initially, then the rats were sacrificed by collecting abdominal aorta blood. Then the livers were also collected. For the plasma samples, the supernatants were separated after centrifugation at 8000 rpm for 5 min at 4℃. The samples were placed at −80 °C to analysis. The blank group (n=5) was treated with 0.5% CMC-Na of the same dosage, and with same operations. The type of anticoagulant was same as what was used in **"*2.2.1 Metabolism Study"***

2.3 Samples Preparation

2.3.1 Metabolism Analysis

Methanol (1:5,v/v) was mixed in blood, bile, urine, gastrointestinal contents and vortexed for 5 min and then centrifuged at 18000 rpm for 10 min at 4 °C. The supernatant was then transferred and dried. The residues were reconstituted with 50% methanol-water, vortexed and centrifuged for 5 min each. The supernatant at each time point was enriched, and vortexed and centrifuged again with the same parameters. Then, the precipitations were reconstituted with methanol-water (1:1) of 150 μL and centrifuged with the same parameters. Finally, the supernatants (80 μL) were transfered into autosampler vials for analysis.

The dried fecal samples were mixed with methanol (1:5, v/v) and then were treated via ultrasonic twice, 0.5 h for each time. The tissue samples were homogenized with the volume of physiological saline water(1 g：3 ml). Then the process method of these two groups was consistent with that of blood.

2.3.2 Pharmacokinetics Analysis

The plasma samples were mixed with acetonitrile (1:5), at the same time,5 μL naringin (NAR) was added into the sample as the inside standard (IS, 5 μg/mL), then vortexed for 5 minutes and centrifuged at18000 rpm for 10 min at 4 °C. The supernatants were collected and blow-dried with a nitrogen blower.

DMD Fast Forward. Published on October 17, 2024 as DOI: 10.1124/dmd.124.001817
This article has not been copyedited and formatted. The final version may differ from this version.

Then they were redissolved by 100 μL methanol then vortexed and centrifuged with the same parameters. Finally, 80 μL supernatants were taken for analysis. The liver samples were processed using the same method as ***"2.3.1 Metabolism Analysis"***.

2.4 Qualitative Analysis Using HPLC-Q-TOF-MS/MS

For the silybin metabolism in rats, a qualitative method was formed by HPLC-Q-TOF system. The column was Waters X Select Hss T3 (3.5 μm, 150×4.6 mm, USA). The mobile phase water was consisted with (0.1% formic acid) of A and acetonitrile of B. The gradient elution is as follow: 0−4.0 min (5% B)、4.0−10.0 min (5% −40% B), 10.0− 20.0 min (40% −65% B), 20.0−22.0 min (65% B), 22.0−23.0 min (65%−90% B), 23.0− 28.0 min (90% B), 28.0−29.0 min (90%−5% B); temperature: 40 ℃ and the injection volume was 10 μL. The Q-TOF mass spectrometer was from AB Sciex with 5600 System and an electrospray ionization (ESI) source (Framingham, MA, USA) equipping the Shimadzu HPLC-30A system (Kyoto, Japan). Scan mode was information-dependent acquisition (IDA) of positive and negative mode. The scan range of MS and MS/MS was *m/z* 100-1300 Da; temperature: 550 ℃; GS1, 55 psi; GS2, 60 psi; decluttering potential (DP), 70 V; The corresponding collision energy (CE), 10 eV; GS1, 55 psi; GS2, 60 psi; curtain gas, 30 psi; spray voltage: 5500 V(ESI+) and -4500 V(ESI-); APCI calibration solutions were injected to real-time calibrate the Q-TOF system for every five samples. Analyst TF 1.6.1 and PeakView 2.0 software (AB SCIEX, MA, USA) was used to analyze the data.

2.5 Quantitative Analysis Using HPLC-Triple Quadrupole MS/MS

To figure out the liver disposition of silybin, new quantitative methods was established to determine the silybin concentration in rat plasma and livers, the results of the analysis method validation were shown in the Appendix (Supp. Table 3-11, Supp. Figure 2). Samples were analyzed by the Sciex API 4000 triple

DMD Fast Forward. Published on October 17, 2024 as DOI: 10.1124/dmd.124.001817
This article has not been copyedited and formatted. The final version may differ from this version.

quadrupole mass spectrometer (Redwood City, CA, USA) with an ESI source and the column was same as that in qualitative step. Ion spray voltage, -4500 V; ion source Gas 1, 55 psi; Gas 2, 60 psi; ion spray temperature, 550 °C; collision gas, 10 Pa and curtain gas, 30 psi. *m/z* 481.0 → 301.1 of silybin and *m/z* 579.4 → 271.2 of Naringin (internal standard, IS) for the negative multiple-reaction monitoring (MRM) fragmentation transitions. CE, 29, 45, (eV) and DP, 92, 96 (V) were set for silybin and IS each. The Analyst 1.5.1 software was used to control the whole system (LC−MS/MS).

2.6 Data processing

WinNonlin software version 8.1.0 (CERTARA, USA) was utilized to calculate the parameters of silybin. The hepatic first-pass effect of silybin was calculated as follows:

$$ER = 100\% * (AUC_{pv} - AUC_{AA})/AUC_{pv} \quad (1)$$

AUC_{pv} and AUC_{AA} stand by the AUC of silybin in the portal vein plasma and abdominal aorta plasma. mean ± standard deviation (SD) was used to illustrate the data. ER stands by the extraction ratio.

3. Results and discussion

3.1 Cleavage pattern of silybin in mass spectrometry

Cleavage way of the protype compound was the basis of identifying its metabolites, we refined the MS and MS/MS spectrums in negative mode based on the previous report(Shibano et al., 2007; Kuki et al., 2012), and the pathway in positive mode were obtained for the first time (Figure 1). As shown in Figure 1A, silybin was detected at 16.826 min in positive mode, $[M + H]^+$ *m/z* 483.1304 ($C_{25}H_{23}O_{10}^+$,3.73 ppm), there were two main pathway of the silybin fragmentation in positive mode. Initially, M0 generated *m/z* 465.1171 by losing H_2O (18 Da), then further generated *m/z* 437.1240 via decarbonylation reaction, the complementary ions *m/z* 257.0434 and *m/z* 163.0751 are derived from *m/z* 437.1240 by breaking D-ring, at

the same time, *m/z* 435.1103 was provided by *m/z* 465.1171 eliminating CH_2OH (31 Da). Additionally, M0 also generated *m/z* 453.1187 via lost CH_2OH (31 Da), then *m/z* 195.0288 was formed by breakage of the C-C bond between B-ring and C-ring, then *m/z* 153.0177 was obtained by losing CH_2(14 Da).

In negative ion mode, as shown in Figure 1B, M0 was eluted at 13.698 min, $[M - H]^-$ *m/z* 481.1147 ($C_{25}H_{21}O_{10}^-$,1.45 ppm). Unlike the positive mode, there were three fragmentation patterns of M0. First M0 occurred decarbonylation reaction CO (28 Da) then generated *m/z* 453.1197, *m/z* 435.1087 was provided by dehydration reactions, *m/z* 257.0457 was derived from breakage of D-ring. Meanwhile, M0 also lost CH_2OH (31 Da) to obtain *m/z* 451.1045, then *m/z* 301.0358 was from D-ring breaking, *m/z* 273.0414 was generated by lost carbonyl, the *m/z* 151.0037 was obtained from the breakage of B-ring and C-ring, then *m/z* 125.0246 was provided by lost carbonyl. Finally, M0 lost a H_2O (18 Da) and generated *m/z* 463.1044, and *m/z* 283.0256 was from breakage of D-ring.

3.2 Metabolite pathway of silybin in *vivo*

A new HPLC-Q-TOF-MS/MS method was established and was used to analyze the bio-samples: the abdominal aorta plasma, hepatic portal vein plasma, hearts, livers, spleens, lungs, kidneys, stomach, ileal, cecum, colon, gastric contents, ileal contents, cecal contents, colon contents, bile, urine, and feces. 32 metabolic pathways and 59 metabolites were identified by comparing with the blank group (Figure 3). And the Extracted Ion Chromatogram (XIC) of all the metabolites were shown in the Figure2

Parent compound (M0)

M0 was detected at 13.69 min, presented a negative ion at *m/z* 481.1147 ($C_{25}H_{21}O_{10}^-$, 1.45 ppm). The retention time, characteristic ions were consistent with the silybin standard. Therefore, M0 was regarded as silybin.

DMD Fast Forward. Published on October 17, 2024 as DOI: 10.1124/dmd.124.001817
This article has not been copyedited and formatted. The final version may differ from this version.

M1

M1 was eluted at 13.83 min, showed a deprotonated ion at *m/z* 657.1440 ($C_{31}H_{29}O_{16}^-$, -3.20 ppm) with the increase of 176 Da compared to M0 which suggested an addition of glucuronide group. In Q-TOF MS^2 spectra, M1 lost glucuronide group and generated *m/z* 481.1141, then *m/z* 453.1197 was derived from the elimination of carbonyl. The *m/z* 301.0359, *m/z* 125.0250 were provided by the breakage of D-ring. These characteristic ions were consistent with that in M0, so M1 was identified as glucuronidation metabolite of silybin.

M2

M2 was found at 13.13 min and detected at *m/z* 737.1053 ($C_{31}H_{29}SO_{19}^-$, 3.26 ppm) in negative mode. In MS/MS spectra, two cleavage patterns were observed: M2 initially produced *m/z* 657.1503 via lost sulfate group, then provided *m/z* 481.1141 by removal of glucuronide group, which matched to M0. At the same time, M2 firstly lost glucuronide group then the sulfate group and generated *m/z* 561.0736, *m/z* 481.1141, which was also consistent with M0. After that, feature fragmentation *m/z* 301.0357 was derived from *m/z* 481.1141 by the breakage of D-ring. So M2 was regarded as glucuronidation and sulfate metabolite of M0. And the catalases are the UGT and the sulfatase

M3-M5

M3 was detected at 16.78 min, presented *m/z* 465.1175 ($C_{25}H_{21}O_9^+$, -1.07 ppm) in positive mode. In Q-TOF MS^2 spectra, the characteristic ion was detected at *m/z* 447.1071 with decrease of 18 Da compared to that of M3, which suggested the H_2O (18 Da) was lost. Meanwhile, M3 produced *m/z* 435.1088 by removal of CH_2OH (31 Da), then *m/z* 257.0440 was formed by D-ring splitting, which was consistent with the feature ion of M0. So M3 was identified as dehydration metabolite of M0. M4, M5 possessed same

DMD Fast Forward. Published on October 17, 2024 as DOI: 10.1124/dmd.124.001817
This article has not been copyedited and formatted. The final version may differ from this version.

cleavage pattern and feature ions. However, the retention time were inconsistent, which was determined as the dehydration metabolite isomers of silybin.

M6

M6 was extracted at 15.62 min, displayed a protonated ion at *m/z* 469.1143 ($C_{24}H_{21}O_{10}^{+}$, 2.98 ppm). As it is shown in Q-TOF MS^2 spectra, *m/z* 451.1050 was derived from dehydration reaction, which was 14 Da lower than M0. It can be inferred that there is a loss of methyl in D-ring. Meanwhile, two feature ions *m/z* 195.0293 and *m/z* 153.0182 were provided via the C-C bond between B-ring and C-ring broke up, which was identical with that of M0. Therefore, M6 was assumed as demethylation metabolite of silybin.

M7

M7 was separated at 19.00 min, the XIC of M7 was at *m/z* 465.1196 in negative mode whose chemical formula was ($C_{25}H_{21}O_{9}^{-}$, 1.07 ppm). M7 generated *m/z* 435.1088 by dropping CH_2OH, then *m/z* 285.0414 was detected through D-ring broke up. These two characteristics ions were 16 Da less than that of M0, which can be speculated that M7 eliminated the ortho- hydroxyl of carbonyl in C-ring. Additionally, the fragmentation ion *m/z* 151.0040 was same as that of M0. So M7 was the dehydroxylation metabolite of M0.

M8

M8(eluted at 16.76 min) formed a deprotonated ion at *m/z* 451.1029 ($C_{24}H_{19}O_{8}^{-}$, -1.33 ppm). As it is presented in MS^2 spectra, the carbonyl in C-ring was removed, then the characteristics ion *m/z* 451.1029 was generated which was 30 Da less than that of M0. It was suggested that M0 occurred dehydroxymethyl reaction. At the same time, M8 formed *m/z* 301.0354、*m/z* 125.0236 via D-ring broke. Therefore, M8 was the dehydroxymethyl metabolite of M0.

DMD Fast Forward. Published on October 17, 2024 as DOI: 10.1124/dmd.124.001817
This article has not been copyedited and formatted. The final version may differ from this version.

M9

M9 was extracted at 19.46 min in the XIC of *m/z* 523.1220 ($C_{27}H_{23}O_{11}^-$, -4.97 ppm). In MS^2 spectra, the base peak, *m/z* 463.1054, was 60 Da less than the molecular ion peak which suggested that there is an acetyl group attaching to the C-ring and it was removed with a water molecular (18 Da). Then M9 produced *m/z* 435.1085 by eliminating carbonyl in C-ring, then C-ring broken and *m/z* 125.0242 was produced, which was consistent with that of M0. So, M9 was identified as acetylation metabolite of silybin.

M10

M10 (extracted at 17.19 min) was in the XIC of *m/z* 453.1187 ($C_{24}H_{21}O_9^-$, -0.88 ppm). The molecular ion peak was less 28 Da than M0 and was also consistent with the fragmentation of M0, which was speculated as the loss of CO (28 Da). At the same time, the base peak *m/z* 407.2801 was 46 Da less than the molecular ion peak indicating the carbonyl and the hydroxyl were eliminated simultaneously. Additionally, *m/z* 125.0230 was from cracks of C-ring. Therefore, M10 was decarbonylation of M10 .

M11

M11 presented a negative ion at *m/z* 435.1082 ($C_{24}H_{19}O_8^-$, -0.69 ppm) in the XIC of 16.83 min. The molecular ion peak matched the characteristics ion of M0. It could be primarily determined as the decarbonylation and dehydration metabolite of M0. Apart from that, D-ring cracked then *m/z* 273.0403 was separated, *m/z* 125.0232 emerged by the breakage of C-ring, which were consistent with that of M0. So, the inference that M11 was the decarbonylation and dehydration metabolite of M0 was further confirmed.

M12-M22

M12 (eluted at 12.48 min) was in the XIC of *m/z* 509.1443 ($C_{27}H_{25}O_{10}^+$, 0.2 ppm). In MS^2 spectra, the

base peak *m/z* 179.0335 was provided by the Carbon-Carbon bond between B-ring and C-ring cracking. It was 16 Da less than M0 indicating the removal of hydroxyl in A or C-ring. Besides, M12 eliminated H_2O (18 Da) to generated *m/z* 491.1344, then the methoxy in D-ring was removed, feature ions *m/z* 461.1241 was found, which was 26 Da more than the corresponding ions of M0. It demonstrated that acetylation reaction occurred in B or D-ring. Additionally, D-ring cracked then *m/z* 163.0747 was obtained. So M12 was regarded as dehydroxylation and acetylization metabolite of M0. M12-M22 possessed same precursor ion and product ions However, the retention time were inconsistent and were assumed as isomers of M12.

M23

M23 (detected at 13.89 min) presented a protonated ion at *m/z* 676.1875 ($C_{31}H_{34}NO_{16}^+$, 0.44 ppm). In MS/MS spectra, *m/z* 659.1609 was 17 Da less than molecular ion peak demonstrating the amino connected to the carbonyl in C-ring was removed. The base peak *m/z* 483.1293 was 176 Da less than *m/z* 659.1609 indicating glucuronide group conjunction. Then the base peak provided *m/z* 465.1180 and *m/z* 163.0748 which were consistent with the characteristic ions of M0. So M23 was determined as glucuronidation and amination metabolite of silybin.

M24-M33

M24 was observed at 11.75 min and shown a positive ion in the XIC of *m/z* 495.1284 ($C_{26}H_{23}O_{10}^+$, -0.40 ppm). In MS/MS spectra, the base peak *m/z* 477.1183 was 18 Da lower than molecular ion peak indicating the removal of water molecule (H_2O, 18 Da), which was consistent with the cleavage pathway of M0. The characteristics ion *m/z* 447.1081 was separated from base peak by eliminating methoxy with 12 Da increase compared to that of M0. Additionally, M24 generated *m/z* 163.0738 by breakage of D-ring which matched the feature ion of M0. It was determined that M24 was dehydroxylation and acylation

DMD Fast Forward. Published on October 17, 2024 as DOI: 10.1124/dmd.124.001817
This article has not been copyedited and formatted. The final version may differ from this version.

metabolite of M0. The molecular ions and product ions of M25-M33 was similar but a different retention time to M24. So, they can be verified as the dehydroxylation and acylation metabolite isomers of silybin.

M34

M34 (extracted at 13.16 min) shown a protonated ion at *m/z* 477.1171 ($C_{26}H_{21}O_9^+$, -1.89 ppm) which was consistent with the base peak of M24. It was 18 Da lower than M24 which suggested the elimination of H_2O. At the same time, the molecular ion peak of M34 provided *m/z* 163.0743 which was consistent with that of M24. So M34 was identified as dehydration metabolite of M24, the dehydroxylation, acylation, and dehydration metabolite of M0.

M35

M35 (observed at 15.15 min) was in the XIC of *m/z* 471.1293 ($C_{24}H_{23}O_{10}^+$, 1.49 ppm). *m/z* 149.0599 was produced by D-ring breaking which was 14 Da lower than that of M0. It was speculated the loss of methyl. Then *m/z* 149.0599 eliminated C_2H_4 and provided the base peak *m/z* 123.0438. Meanwhile, the characteristic ion *m/z* 259.0603 was 2 Da higher than that of M0. Therefore, M35 was the demethylation and hydrogenation metabolite of silybin standard.

M36, M37, M38

M36 was detected at 19.00 min, shown a deprotonated ion at *m/z* 479.0998 ($C_{25}H_{19}O_{10}^-$, 2.92 ppm). The base peak *m/z* 299.0210 and *m/z* 271.0259 which was provided by base peak were 2 Da lower than that of M0. It indicated that dehydrogenation reaction occurred. At the same time, *m/z* 151.0041 was generated by base peak, which was consistent with the feature ion of M0. So M36 was dehydrogenation metabolite of silybin standard. M37, M38 owned similar molecular ions and product ions, but a different retention time to M36, which can be verified as the dehydrogenation metabolite of silybin isomers.

DMD Fast Forward. Published on October 17, 2024 as DOI: 10.1124/dmd.124.001817
This article has not been copyedited and formatted. The final version may differ from this version.

M39

M39 was eluted at 15.21 min, a negative ion was separated at *m/z* 469.1150 ($C_{24}H_{21}O_{10}^-$, 2.13 ppm), the base peak *m/z* 285.0413 was derived from breakage of D-ring, with 16 Da loss. It was speculated as dehydration reaction. Then M39 lost H_2O and CO provided *m/z* 423.2769 with 12 Da less than that of M0 which suggested double hydrogenation reactions occurred based on dehydration reaction. Besides, fragment *m/z* 125.0243 was also consistent with that of M0. So M39 was dehydroxylation and double hydrogenation metabolite of M0.

M40

M40(detected at 15.29 min), was shown in the XIC of *m/z* 537.1400 ($C_{28}H_{25}O_{11}^+$, 1.68 ppm). In Q-TOF MS2 spectra, the molecular ion peak and base peak (*m/z* 519.1293) was consistent with the feature fragments of M42 and was 30 Da less than M42. It indicated that hydroxymethyl was removed. Besides, *m/z* 163.0746 was provided by cracks of D-ring which matched the characteristic ion of M0. It can be determined that the eliminated hydroxymethyl was in C-ring. So M40 was the acetylization, vinylation, hydroxylation and dehydroxymethylation of M0.

M41

M41 was extracted at 13.19 min, its molecular ion peak was at $[M+H]^+$ *m/z* 551.1581 ($C_{29}H_{27}O_{11}^+$, 2.18 ppm). In Q-TOF MS^2 spectra, the base peak *m/z* 221.0449 was 26 Da more than the characteristic ion of M0. It indicated that the vinylation reaction happened in A-ring or C-ring. *m/z* 533.1481、*m/z* 515.1368 were derived from the continuous loss of two water molecules. Then the hydroxymethyl dropped off and the feature fragment *m/z* 485.1232 was generated with the 68 Da increase of that of M0. It demonstrated the acetylation reaction occurred in B-ring or D-ring based on the ethylene reaction. At the same time, *m/z*

DMD Fast Forward. Published on October 17, 2024 as DOI: 10.1124/dmd.124.001817
This article has not been copyedited and formatted. The final version may differ from this version.

163.0752 was same as the fragments of M0. So M41 ought to be the vinylation and acetylation metabolite of silybin.

M42

M42 was observed at 12.96 min. its protonated ion was at *m/z* 567.1513 ($C_{29}H_{27}O_{12}^{+}$, 2.82 ppm). In Q-TOF MS^2 spectra, the characteristic ion *m/z* 237.0394 was provided by the breakage of B-ring and C-ring, which was 42 Da more than that of M0. It suggested the acetylization reaction happened in A-ring or C-ring. At same time, *m/z* 549.1391, *m/z* 519.1319 and *m/z* 491.1337 were obtained after sequential loss of H_2O, CH_2OH and CO. These ions were 84 Da more than that of M0. It indicated the vinylation and hydroxylation reactions occurred based on the acetylization reaction. Additionally, *m/z* 163.0758 was also consistent with the feature ion of M0. So M42 was the acetylization, vinylation and hydroxylation metabolite of silybin standard.

M43-M53 M57-M59

M43 was detected at 13.64 min, a positive ion was obtained at *m/z* 676.2047 ($C_{35}H_{34}NO_{13}^{+}$, 3.25 ppm), with the base peak of *m/z* 495.1303. It was 181 Da less than M24 which was referred as the loss of tyrosine, then *m/z* 477.1194 was generated and was identical to M24. It indicated the tyrosine was connected to the carbonyl of C-ring. Therefore, M43 was tyrosine metabolite of M24 and the dehydroxylation, acylation and tyrosine metabolite of M0. M44 possessed same molecular ion and product ions but different retention time and were assumed as isomers of M43. Additionally, the base peaks of M45-M53 M57-M59 were same as M43 but with different molecular peaks. Also, their characteristic ions were consistent with that of M24, which can be identified as the metabolites based on the M24 the acetylization and vinylation metabolite of M0. The data were shown in Table 1.

DMD Fast Forward. Published on October 17, 2024 as DOI: 10.1124/dmd.124.001817
This article has not been copyedited and formatted. The final version may differ from this version.

M54

M54 was detected at 13.13 min, the molecular ion peak was *m/z* 642.1853 ($C_{31}H_{32}NO_{14}^+$, 2.80 ppm). In Q-TOF MS^2 spectra, the base peak *m/z* 567.1516 was 75 Da more than molecular ion peak which was speculated that the glycine bonded on the carbonyl of C-ring was lost. At the same time, the base peak *m/z* 567.1516 and feature ion *m/z* 519.1300 was consistent with M42. So M54 was the glycine metabolite of M42 which is the acetylization, vinylation and hydroxylation and glycine metabolite of silybin standard.

M55-M56

M55 (eluted at 14.55 min) was in the XIC of *m/z* 640.2399 ($C_{33}H_{38}NO_{12}^+$, 1.56 ppm). In Q-TOF MS^2 spectra, the base peak *m/z* 509.1462 was 131 Da less than molecular ion peak which indicating the loss of leucine located at the carbonyl of C-ring. At the same time, the product ions *m/z* 509.1462，*m/z* 491.1349 and *m/z* 163.0748 was consistent with M12. So M55 was the leucine metabolite of M16 and the dehydroxylation, acetylization, leucine metabolite of M0. Additionally, the product ion of M56 was same as that of M55 and the base peak was 117 Da less than the molecular peak which indicating the valine was lost. So M56 was the dehydroxylation, acetylization, valine metabolite of M0.

3.3 Pharmacokinetics Studies

The pharmacokinetic curve of silybin in abdominal aorta and hepatic vein plasma after oral administration with 200 mg/kg were presented in Figure 4. As it was shown in the figure, the concentration of silybin in abdominal aorta reached the C_{max} which was 54249.66±31539.88 ng/mL rapidly at T_{max} of 0.29±0.08 h. Then drug-time curve of silybin in the hepatic portal vein had the similar trend as that in abdominal aorta. However, the AUC of silybin in hepatic portal vein (72004.25±30734.69 ng/mL*h) was multiples times higher than that in abdominal aorta (25364.72±14 ng/mL*h). As a result, the ER was

DMD Fast Forward. Published on October 17, 2024 as DOI: 10.1124/dmd.124.001817
This article has not been copyedited and formatted. The final version may differ from this version.

acquired as 63.30 % for silybin by calculating which indicated that large amounts of silybin may be accumulated in the liver. Moreover, the corresponding PK parameters were presented in Table 2. At the same time, the distribution of silybin in the livers has also been determined. The drug-time curve has been shown in the Figure.5, at 0.50±0.34 h the silybin concentration in the liver reach the peak value which was as high as 120.26±38.35 μg /kg (C_{max}). The other related parameters were also shown in Table 2.

3.4 Discussion

In this work, metabolism characteristic of silybin in rats was systematically evaluated. Firstly, based on the previous report (Shibano et al., 2007), the pathway of silybin in negative mode was refined, and the pathway in positive mode was obtained for the first time. Totally, 32 metabolism pathways and 59 metabolites were detected (Supp. Figure. 1) including dehydration, dehydroxylation, decarbonylation, dehydroxymethylation, glucuronidation, sulfation, acetyation, acylation and amino acid binding and other I., II phase reactions and corresponding compound reactions (Table 1). Within these reactions, the glucuronidation reaction was catalyzed by UGT transferase in the liver (Charrier et al., 2014). Except for metabolic reactions catalyzed by endogenous bioenzymes, most of the metabolites are found in the gut due to the presence of a rich microbiota in the gut, and it has been demonstrated that the complete metabolism of flavonoid in the gut requires the close involvement of enterobacteria. Aromatic amino acid reactions may be related to *Eubacterium hallii, and Clostridium barlettii*, Demethylation reactions may be catalyzed by *Butyribacterium methylotrophicum and Eubacterium callanderi*, Dehydroxylation may be associated with *Clostridium scindens and Eggerthella lenta*. These floras have a close interaction with the drug and produce a rich metabolic response to the drug. (Rowland et al., 2018; Zimmermann et al., 2019; Pant et al., 2023) The question as to whether these metabolites will have a positive regulatory effec deserves further

study in the future.

In our study, only 2 metabolites (M1, M23) were found in abdominal aorta plasma and hepatic portal vein plasma of rats after administrating silybin orally. In the liver（M1）, lung（M1）, bile（M2） and urine（M3）, only 1 metabolite was observed. And 2 metabolites were detected in the abdominal aorta and hepatic portal vein each. No metabolites could be found in the brain, heart, spin, spleen and kidney. And the protype metabolite could not be found in the spin and spleen (Supp. Table. 2). The compounds we identified in plasma, most organs and tissues were consistent with what has been reported in the literature (Hoh et al., 2007; Marhol et al., 2015; Xu et al., 2022)

However, there are interesting findings in the tissues of the gastrointestinal tissues as well as in the corresponding contents. 25 metabolites were identified in gastric, ileal, 16 in cecum and 9 in colon tissues, at the same time, 12, 32 and 34 metabolites were confirmed in corresponding contents. Among these metabolites M5 and M9-M10 were specific to the gastric contents, M12, M16-M17 and M19-M20 were specific to the ileum contents, M4, M8, M11, M14-M15, M18, M22, M25-M26, M28-M29, M35, M40, M42, M53-M54 and M56-M59 were specific to the cecum contents, M4, M6-M9, M24-M28, M30-M36, M46-M47, M49, M53 and M56-M59 were specific to the colon contents. 21 metabolites were found in the feces, which indicates silybin was mainly excreted by feces. As it is shown in Supp. Figure1 the metabolites identified in gastrointestinal tract possessed 88% of all (52 out of 59).

In contrast to only one metabolite (M1) found in the liver, silybin undergoes abundant metabolic reactions in the intestine. It indicates us that intestine is the main metabolic site of silybin and not its main target organ, the liver. To further determine the hepatic disposition of silybin, we determined the hepatic first-pass effect of silybin by LC-MS/MS, which showed that the first-pass effect was as high as 63.30±

13.01%, while only one metabolite was found. And at the same time, we further conformed the concentration of silybin in the livers. As shown in the result, high concentrations of silybin in the livers suggested abundant silybin was stored in the liver.

As the most important metabolic organs, livers were the main metabolic places of many drugs, but the above experimental results proved that the gastrointestinal tract is the main metabolizing organ of silybin in rats. Meanwhile, intestinal bacteria were also closely involved in the metabolic process of silybin as a novel metabolic organ. It was probably because the intestinal microbiota contains many various types of enzymes, including several hydrolases such as glycosidases, glucuronidases, sulfate esterases, amidases and esterases. In addition the microbial enzymes catalyze various types of reactions including oxidation, reduction, decarboxylation, demethylation, isomerization, and ring cleavage (Hervert-Hernández and Goñi, 2011), resulting in a wide range of metabolisms of silybin once it enters the gut.

Additionally, silybin's role in disease modulation in the gut has also been explored in several related studies. For example, in Alzheimer's disease research, Silybin has been shown to have a positive effect on the disease by modulating intestinal bacteria (Shen et al., 2019). It also acts as a hepatoprotective drug and can have an intervention effect on Non-alcoholic fatty liver disease (NAFLD) by affecting the composition of intestinal bacteria (Li et al., 2020). These studies also illustrate the very close interaction of silybin with intestinal tissues as well as intestinal contents.

In conclusion, in this work, after oral administration of silybin to rats, 29 (out of 32, Supp. Table. 1) metabolic pathways and 56 (out of 59, Supp. Table. 2) metabolites were identified for the first time. Of note is that most of the metabolites were derived from intestinal tissues as well as intestinal contents (52 out of 59, Supp. Figure1). This finding suggests that the gastrointestinal tract may be the main metabolic

DMD Fast Forward. Published on October 17, 2024 as DOI: 10.1124/dmd.124.001817
This article has not been copyedited and formatted. The final version may differ from this version.

site of silybin rather than its main target organ, the liver. For the first time, the gastrointestinal tract was determined as the unnoticed metabolic organ. To further verify our conjecture, we investigated the hepatic first-pass effect of silybin in rats, and the results showed that the hepatic first-pass effect of silybin was as high as 63.30±13.01%. At the same time, the high concentration of silybin also indicates it was accumulated in the liver rather than metabolized, these findings also provide a solid material basis for the in-depth study of silybin and its rational use in clinical practice.

References

Abenavoli L, Greco M, Nazionale I, Peta V, Milic N, Accattato F, Foti D, Gulletta E, and Luzza F (2015) Effects of Mediterranean diet supplemented with silybin-vitamin E-phospholipid complex in overweight patients with non-alcoholic fatty liver disease. *Expert Rev Gastroenterol Hepatol* **9:**519–527 doi: 10.1586/17474124.2015.1004312.

Abourashed EA, Mikell JR, and Khan IA (2012) Bioconversion of silybin to phase I and II microbial metabolites with retained antioxidant activity. *Bioorg Med Chem* **20:**2784–2788 doi: 10.1016/j.bmc.2012.03.046.

Bai Y, Chen L, Cao Y-F, Hou X-D, Jia S-N, Zhou Q, He Y-Q, and Hou J (2021) Beta-Glucuronidase Inhibition by Constituents of Mulberry Bark. *Planta Med* **87:**631–641 doi: 10.1055/a-1402-6431.

Bijak M (2017) Silybin, a Major Bioactive Component of Milk Thistle (Silybum marianum L. Gaernt.)-Chemistry, Bioavailability, and Metabolism. *Molecules* **22** doi: 10.3390/molecules22111942.

Charrier C, Azerad R, Marhol P, Purchartová K, Kuzma M, and Křen V (2014) Preparation of silybin phase II metabolites: Streptomyces catalyzed glucuronidation. *Journal of Molecular Catalysis B: Enzymatic* **102:**167–173 doi: 10.1016/j.molcatb.2014.02.008.

Gunaratna C and Zhang T (2003) Application of liquid chromatography-electrospray ionization-ion trap mass spectrometry to investigate the metabolism of silibinin in human liver microsomes. *J Chromatogr B Analyt Technol Biomed Life Sci* **794:**303–310 doi:

10.1016/s1570-0232(03)00484-7.

Hervert-Hernández D and Goñi I (2011) Dietary Polyphenols and Human Gut Microbiota: a Review. *Food Reviews International* **27:**154–169 doi: 10.1080/87559129.2010.535233.

Hoh CSL, Boocock DJ, Marczylo TH, Brown VA, Cai H, Steward WP, Berry DP, and Gescher AJ (2007) Quantitation of silibinin, a putative cancer chemopreventive agent derived from milk thistle (Silybum marianum), in human plasma by high-performance liquid chromatography and identification of possible metabolites. *J Agric Food Chem* **55:**2532–2535 doi: 10.1021/jf063156c.

Kuki Á, Biri B, Nagy L, Deák G, Kalmár J, Mándi A, Nagy M, Zsuga M, and Kéki S (2012) Collision induced dissociation study of the major components of silymarin. *International Journal of Mass Spectrometry* **315:**46–54 doi: 10.1016/j.ijms.2012.02.021.

Li X, Wang Y, Xing Y, Xing R, Liu Y, and Xu Y (2020) Changes of gut microbiota during silybin-mediated treatment of high-fat diet-induced non-alcoholic fatty liver disease in mice. *Hepatol Res* **50:**5–14 doi: 10.1111/hepr.13444.

Marhol P, Bednář P, Kolářová P, Večeřa R, Ulrichová J, Tesařová E, Vavříková E, Kuzma M, and Křen V (2015) Pharmacokinetics of pure silybin diastereoisomers and identification of their metabolites in rat plasma. *Journal of Functional Foods* **14:**570–580 doi: 10.1016/j.jff.2015.02.031.

Pant A, Maiti TK, Mahajan D, and Das B (2023) Human Gut Microbiota and Drug Metabolism. *Microb Ecol* **86:**97–111 doi: 10.1007/s00248-022-02081-x.

Pferschy-Wenzig E-M, Kunert O, Thumann T, Moissl-Eichinger C, and Bauer R (2023)

Characterization of metabolites from milk thistle flavonolignans generated by human fecal microbiota. *Phytochemistry* **215:**113834 doi: 10.1016/j.phytochem.2023.113834.

Rowland I, Gibson G, Heinken A, Scott K, Swann J, Thiele I, and Tuohy K (2018) Gut microbiota functions: metabolism of nutrients and other food components. *Eur J Nutr* **57:**1–24 doi: 10.1007/s00394-017-1445-8.

Shen L, Liu L, Li X-Y, and Ji H-F (2019) Regulation of gut microbiota in Alzheimer's disease mice by silibinin and silymarin and their pharmacological implications. *Appl Microbiol Biotechnol* **103:**7141–7149 doi: 10.1007/s00253-019-09950-5.

Shibano M, Lin A-S, Itokawa H, and Lee K-H (2007) Separation and characterization of active flavonolignans of Silybum marianum by liquid chromatography connected with hybrid ion-trap and time-of-flight mass spectrometry (LC-MS/IT-TOF). *J Nat Prod* **70:**1424–1428 doi: 10.1021/np070136b.

Tuli HS, Mittal S, Aggarwal D, Parashar G, Parashar NC, Upadhyay SK, Barwal TS, Jain A, Kaur G, Savla R, Sak K, Kumar M, Varol M, Iqubal A, and Sharma AK (2021) Path of Silibinin from diet to medicine: A dietary polyphenolic flavonoid having potential anti-cancer therapeutic significance. *Semin Cancer Biol* **73:**196–218 doi: 10.1016/j.semcancer.2020.09.014.

Tvrdý V, Pourová J, Jirkovský E, Křen V, Valentová K, and Mladěnka P (2021) Systematic review of pharmacokinetics and potential pharmacokinetic interactions of flavonolignans from silymarin. *Medicinal research reviews* **41:**2195–2246 doi: 10.1002/med.21791.

Wah Kheong C, Nik Mustapha NR, and Mahadeva S (2017) A Randomized Trial of Silymarin for the Treatment of Nonalcoholic Steatohepatitis. *Clin Gastroenterol Hepatol* **15:**1940-1949.e8

511 doi: 10.1016/j.cgh.2017.04.016.

512 Xu C, Yuan Y, Pang P, Yang H, Zhang Q, Yuan D, and Qi W (2022) Urinary excretion of silibinin
513 diastereoisomers and their conjugated metabolites in rat and human at different dosages.
514 *Biomed Chromatogr* **36:**e5480 doi: 10.1002/bmc.5480.

515 Xu F, Yang J, Negishi H, Sun Y, Li D, Zhang X, Hayashi T, Gao M, Ikeda K, and Ikejima T (2018)
516 Silibinin decreases hepatic glucose production through the activation of gut-brain-liver axis in
517 diabetic rats. *Food Funct* **9:**4926–4935 doi: 10.1039/c8fo00565f.

518 Yassin NYS, AbouZid SF, El-Kalaawy AM, Ali TM, Almehmadi MM, and Ahmed OM (2022)
519 Silybum marianum total extract, silymarin and silibinin abate hepatocarcinogenesis and
520 hepatocellular carcinoma growth via modulation of the HGF/c-Met, Wnt/β-catenin, and
521 PI3K/Akt/mTOR signaling pathways. *Biomed Pharmacother* **145:**112409 doi:
522 10.1016/j.biopha.2021.112409.

523 Zhang Y, Yang D-H, Zhang Y-T, Chen X-M, Li L-L, and Cai S-Q (2014) Biotransformation on the
524 flavonolignan constituents of Silybi Fructus by an intestinal bacterial strain Eubacterium
525 limosum ZL-II. *Fitoterapia* **92:**61–71 doi: 10.1016/j.fitote.2013.10.001.

526 Zimmermann M, Zimmermann-Kogadeeva M, Wegmann R, and Goodman AL (2019) Mapping
527 human microbiome drug metabolism by gut bacteria and their genes. *Nature* **570:**462–467
528 doi: 10.1038/s41586-019-1291-3.

529

Authorship contribution

Yuanbo Sun and Like Xie: Participated in research design, Wrote or contributed to the writing of the manuscript, Performed data analysis.

Jing Zhang: Performed data analysis, participated in research design,

Runing Liu, Yanquan Yang, Yapeng Wu, and Hanbing Li: Conducted experiments

Ying Peng and Guangji Wang and Natalie Medlicott: Wrote or contributed to the writing of the manuscript.

Jianguo Sun: Participated in research design, Wrote or contributed to the writing of the manuscript, Performed data analysis.

Conflicts of interest statement

The authors declare that they have no conflicts of interest.

Acknowledgments

We appreciate the support from Leading technology foundation research project of Jiangsu province. (No. BK20192005).

We sincerely thank Jie Zhao and Zhenglin Hao (Animal Experimental Center of China Pharmaceutical University) for their support with animal experiments.

Data Availability Statement Samples

The authors declare that all the data supporting the findings of this study are available within the paper and its Supplemental Data.

DMD Fast Forward. Published on October 17, 2024 as DOI: 10.1124/dmd.124.001817
This article has not been copyedited and formatted. The final version may differ from this version.

Figure Captions

Figure 1. A, B, the extracted ion chromatogram and MS/MS spectra of silybin from negative and positive mode, C, D the possible cleavage pattern of silybin in positive and negative ion modes.

Figure 2. XIC of the silybin metabolites in rat tissues and intestinal contents. X-axis is time in minutes Y-axis is response intensity.

Figure 3. Silybin metabolic pathway in rats after oral administration.

Figure 4. Concentration-time curve of silybin in hepatic vein plasma and abdominal aorta by intragastric administration at 200 mg/kg. (mean ± SD, n = 5). i.g.: intragastric administration; i.g.pv: hepatic portal vein blood collected after intragastric administration.

Figure 5. Concentration of silybin in the liver by intragastric administration at 200 mg/kg. (mean ± SD, n = 5)

Table1. Information of the silybin metabolites in rats after oral administration

NO	t_R/min	Molecular formula	Ion mode	$[M+H]^-/[M+H]^+$			MS/MS (*m/z*)	Metabolite description
				Observed *m/z*	Calculated *m/z*	Error (10^{-6})		
M0	13.69	$C_{25}H_{22}O_{10}$	$[M-H]^-$	481.1147	481.1135	2.49	481.1147; 301.0358;125.0246	Protype
M1[a]	13.83	$C_{31}H_{30}O_{16}$	$[M-H]^-$	657.1440	657.1461	-3.20	481.1141;453.1179;301.0359;125.0250	Glucuronidation
M2[a]	13.13	$C_{31}H_{30}SO_{19}^-$	$[M-H]^-$	737.1053	737.1029	3.26	657.1503;561.0736;481.1141;301.0357	Sulfation + Glucuronidation
M3	16.78	$C_{25}H_{20}O_9$	$[M+H]^+$	465.1175	465.118	-1.07	447.1071;435.1088;257.0440	Dehydration
M4	16.65	$C_{25}H_{20}O_9$	$[M+H]^+$	465.1191	465.118	2.36	447.1069;435.1088;257.0449	Dehydration
M5	14.67	$C_{25}H_{20}O_9$	$[M+H]^+$	465.1194	465.118	3.01	447.1068;435.1232;257.0453	Dehydration
M6[a]	15.62	$C_{24}H_{20}O_{10}$	$[M+H]^+$	469.1143	469.1129	2.98	451.1050;195.0293;153.0182	Demethylation
M7	19.00	$C_{25}H_{22}O_9$	$[M-H]^-$	465.1196	465.1191	1.07	435.1088;285.0414;151.0040	Dehydroxylation
M8	16.76	$C_{24}H_{20}O_8$	$[M-H]^-$	451.1029	451.1035	-1.33	301.0354;125.0236	Dehydroxymethylation
M9	19.46	$C_{27}H_{24}O_{11}$	$[M-H]^-$	523.1220	523.1246	-4.97	463.1054;435.1085;125.0242	Acetylization
M10	17.19	$C_{24}H_{22}O_9$	$[M-H]^-$	453.1187	453.1191	-0.88	407.2801;125.0230	Decarbonylation
M11	16.83	$C_{24}H_{20}O_8$	$[M-H]^-$	435.1082	435.1085	-0.69	273.0403;125.0232	Decarbonylation + Dehydration
M12	12.48	$C_{27}H_{24}O_{10}$	$[M+H]^+$	509.1443	509.1442	0.20	491.1344;461.1241;179.0335;163.0747	Dehydroxylation + Acetylization
M13	13.05	$C_{27}H_{24}O_{10}$	$[M+H]^+$	509.1443	509.1442	0.20	491.1346;461.1388;179.0337;163.0752	Dehydroxylation + Acetylization
M14	13.41	$C_{27}H_{24}O_{10}$	$[M+H]^+$	509.1446	509.1442	0.79	491.1351;461.1250;179.0341;163.0750	Dehydroxylation + Acetylization
M15	13.64	$C_{27}H_{24}O_{10}$	$[M+H]^+$	509.1448	509.1442	1.18	491.1355;461.1246;179.0340;163.0749	Dehydroxylation + Acetylization
M16	13.78	$C_{27}H_{24}O_{10}$	$[M+H]^+$	509.1442	509.1442	0.00	491.1362;461.1253;179.0341;163.0759	Dehydroxylation + Acetylization
M17	14.09	$C_{27}H_{24}O_{10}$	$[M+H]^+$	509.1456	509.1442	2.75	491.1363;461.1254;179.0345;163.0758	Dehydroxylation + Acetylization
M18	14.17	$C_{27}H_{24}O_{10}$	$[M+H]^+$	509.1446	509.1442	0.79	491.1359;461.1253;179.0343;163.0757	Dehydroxylation + Acetylization
M19	14.43	$C_{27}H_{24}O_{10}$	$[M+H]^+$	509.1452	509.1442	1.96	491.1351;461.1247;179.0332;163.0756	Dehydroxylation + Acetylization

M20	14.55	$C_{27}H_{24}O_{10}$	$[M+H]^+$	509.1449	509.1442	1.37	491.1362;461.1249;179.0340;163.0759	Dehydroxylation + Acetylization
M21	15.14	$C_{27}H_{24}O_{10}$	$[M+H]^+$	509.1440	509.1442	-0.39	491.1362;461.1236;179.0335;163.0750	Dehydroxylation + Acetylization
M22	20.20	$C_{27}H_{24}O_{10}$	$[M+H]^+$	509.1444	509.1442	0.39	491.1348;461.1246;179.0331;163.0745	Dehydroxylation + Acetylization
M23	13.89	$C_{31}H_{33}NO_{16}$	$[M+H]^+$	676.1875	676.1872	0.44	659.1609;483.1293;465.1180;163.0748	Glucuronidation + Amination
M24	11.75	$C_{26}H_{22}O_{10}$	$[M+H]^+$	495.1284	495.1286	-0.40	477.1183;447.1081;163.0738	Dehydroxylation + Acylation
M25	12.21	$C_{26}H_{22}O_{10}$	$[M+H]^+$	495.1290	495.1286	0.81	477.1189;447.1081;163.0745	Dehydroxylation + Acylation
M26	12.74	$C_{26}H_{22}O_{10}$	$[M+H]^+$	495.1296	495.1286	2.02	477.1196;447.1072;163.0745	Dehydroxylation + Acylation
M27	12.91	$C_{26}H_{22}O_{10}$	$[M+H]^+$	495.1285	495.1286	-0.20	477.1193;447.1080;163.0746	Dehydroxylation + Acylation
M28	13.07	$C_{26}H_{22}O_{10}$	$[M+H]^+$	495.1284	495.1286	-0.40	477.1189;447.1070;165.0754	Dehydroxylation + Acylation
M29	13.17	$C_{26}H_{22}O_{10}$	$[M+H]^+$	495.1284	495.1286	-0.40	477.1183;447.1071;163.0743	Dehydroxylation + Acylation
M30	13.55	$C_{26}H_{22}O_{10}$	$[M+H]^+$	495.1287	495.1286	0.20	477.1201;447.1071;163.0748	Dehydroxylation + Acylation
M31	13.89	$C_{26}H_{22}O_{10}$	$[M+H]^+$	495.1283	495.1286	-0.61	477.1183;477.1083;163.0757	Dehydroxylation + Acylation
M32	14.04	$C_{26}H_{22}O_{10}$	$[M+H]^+$	495.1292	495.1286	1.21	477.1190;447.1090;163.0744	Dehydroxylation + Acylation
M33	17.16	$C_{26}H_{22}O_{10}$	$[M+H]^+$	495.1289	495.1286	0.61	477.1183;447.1096;163.0746	Dehydroxylation + Acylation
M34	13.16	$C_{26}H_{20}O_9$	$[M+H]^+$	477.1171	477.1180	-1.89	163.0743	Dehydroxylation + Acylation+ Dehydration
M35	15.15	$C_{24}H_{22}O_{10}$	$[M+H]^+$	471.1293	471.1286	1.49	259.0603;149.0599;123.0438	Demethylation +Hydrogenation
M36	19.00	$C_{25}H_{20}O_{10}$	$[M-H]^-$	479.0998	479.0984	2.92	299.0210;271.0259;151.0041	Dehydrogenation
M37	19.26	$C_{25}H_{20}O_{10}$	$[M-H]^-$	479.0995	479.0984	2.30	299.0211;271.0258; 151.0045	Dehydrogenation
M38	19.67	$C_{25}H_{20}O_{10}$	$[M-H]^-$	479.0981	479.0984	-0.63	299.0214;271.0266; 151.0037	Dehydrogenation
M39	15.21	$C_{24}H_{22}O_{10}$	$[M-H]^-$	469.1150	469.1140	2.13	423.2769;285.0413;125.0243	Dehydroxylation +2 X Hydrogenation
M40	15.29	$C_{28}H_{24}O_{11}$	$[M+H]^+$	537.1400	537.1391	1.68	537.1400;519.1293;163.0746	Acetylization + Vinylation + Hydroxylation+ Dehydroxymethylation
M41	13.19	$C_{29}H_{26}O_{11}$	$[M+H]^+$	551.1581	551.1548	2.18	533.1481;515.1368; 485.1232; 221.0449; 163.0752	Acetylization + Vinylation
M42	12.96	$C_{29}H_{26}O_{12}$	$[M+H]^+$	567.1513	567.1497	2.82	549.1391;519.1319;491.1337;237.0394;163.0758	Acetylization + Vinylation + hydroxylation

M43	13.64	$C_{35}H_{33}NO_{13}$	$[M+H]^+$	676.2047	676.2025	3.25	495.1303;477.1194	Dehydrolyzation + Acylation + Tyrosine
M44	13.49	$C_{35}H_{33}NO_{13}$	$[M+H]^+$	676.2022	676.2025	-0.44	495.11282;477.1174	Dehydrolyzation + Acylation + Tyrosine
M45	14.33	$C_{35}H_{33}NO_{12}$	$[M+H]^+$	660.2104	660.2076	4.24	495.1312;477.1211	Dehydrolyzation + Acylation + Phenylalanine
M46	14.18	$C_{31}H_{33}NO_{12}$	$[M+H]^+$	660.2104	660.2076	4.24	495.1303;477.1188	Dehydrolyzation + Acylation + Phenylalanine
M47	13.80	$C_{31}H_{33}NO_{12}S$	$[M+H]^+$	644.1846	644.1796	3.73	495.1307;477.1190	Dehydrolyzation + Acylation+ Methionine
M48	13.69	$C_{31}H_{33}NO_{12}S$	$[M+H]^+$	644.1840	644.1796	1.55	495.1288;477.1187	Dehydrolyzation + Acylation+ Methionine
M49	13.13	$C_{31}H_{31}NO_{14}$	$[M+H]^+$	642.1824	642.1817	1.09	495.1309;477.1195	Dehydrolyzation + Acylation + Glutamic acid
M50	14.03	$C_{32}H_{35}NO_{12}$	$[M+H]^+$	626.2246	626.2232	1.76	495.1294;477.1189	Dehydrolyzation + Acylation + Leucine
M51	13.88	$C_{32}H_{35}NO_{12}$	$[M+H]^+$	626.2233	626.2232	0.16	495.1297;477.1187	Dehydrolyzation + Acylation + Leucine
M52	13.57	$C_{31}H_{31}NO_{12}$	$[M+H]^+$	610.1939	610.1919	3.28	495.1303;477.1196	Dehydrolyzation + Acylation + Proline
M53	13.18	$C_{29}H_{29}NO_{12}$	$[M+H]^+$	584.1788	584.1763	4.28	495.1316;477.1204	Dehydrolyzation + Acylation + Alanine
M54	13.13	$C_{31}H_{31}NO_{14}$	$[M+H]^+$	642.1853	642.1817	2.80	567.1516;519.1300	Acetylization + Vinylation +Hydroxylation + Glycine
M55	14.55	$C_{33}H_{37}NO_{12}$	$[M+H]^+$	640.2399	640.2389	1.56	509.1462;491.1349;163.0748	Dehydroxylation + Acetylization + Leucine
M56	13.37	$C_{32}H_{35}NO_{12}$	$[M+H]^+$	626.2248	626.2232	2.55	509.1464;491.1356;163.0750	Dehydroxylation + Acetylization + Valine
M57	13.06	$C_{28}H_{29}NO_{10}$	$[M+H]^+$	540.1885	540.1864	3.89	495.1321;477.1210	Dehydrolyzation + Acylation + Ethylamino
M58	12.89	$C_{27}H_{27}NO_{10}$	$[M+H]^+$	526.1730	526.1708	4.18	495.1315;477.1207	Dehydrolyzation + Acylation + Methylamination
M59	13.40	$C_{30}H_{31}NO_{10}$	$[M+H]^+$	566.2030	566.2021	1.59	495.1309;477.1198	Dehydrolyzation + Acylation + Pyrrolidine

[a] reported metabolite of silybin

Table 2. The pharmacokinetic parameters of silybin in abdominal aorta, hepatic vein plasma and livers after intragastric administration at 200 mg/kg (n=5).

Parameter	i.g.[a](200mg/kg)	i.g.pv[b](200mg/kg)	Livers (i.g., 200mg/kg)
C_{max} (ng/mL)	163632.10±80650.23	54249.66±31539.88	120.26±38.35 (μg/kg)
$t_{1/2\beta}$ (h)	0.99±0.23	2.63±1.56[c]	3.01±1.67
T_{max} (h)	0.21±0.08	0.29±0.08	0.50±0.34
AUC_{0-t} (ng/mL*h)	72004.25±30734.69	25364.72±14	171.29±36.00 (μg /kg*h)
ER (%)		63.30±13.01	

`

580 i.g.[a]: intragastric administration; i.g.pv[b:] hepatic portal vein blood collection after intragastric administration; ER: extraction ratio.

581

582

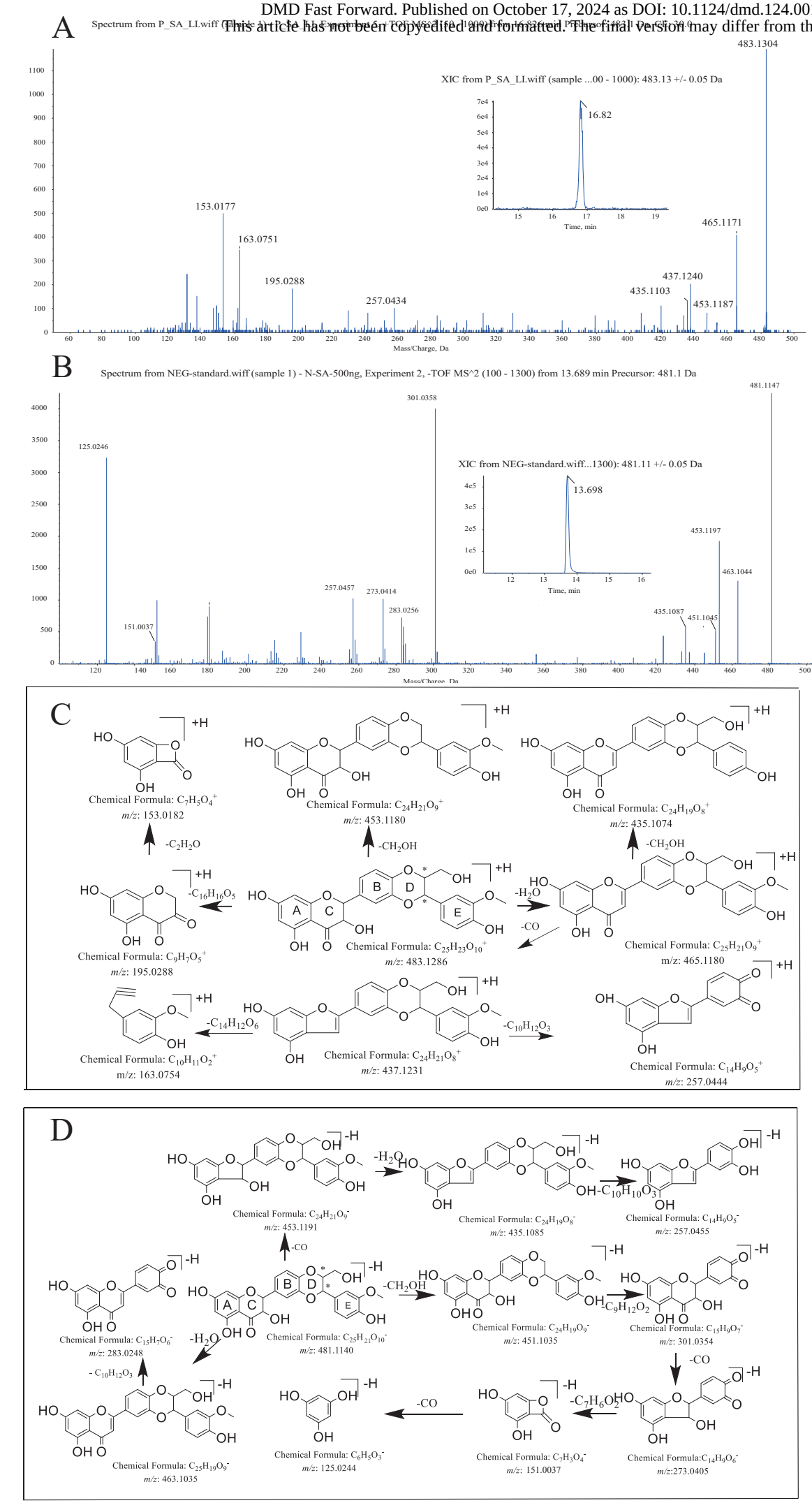

Figure 1. A, B, the extracted ion chromatogram and MS/MS spectra of silybin from negative and positive mode, C, D the possible cleavage pattern of silybin in positive, negative ion modes.

DMD Fast Forward. Published on October 17, 2024 as DOI: 10.1124/dmd.124.001817
This article has not been copyedited and formatted. The final version may differ from this version.

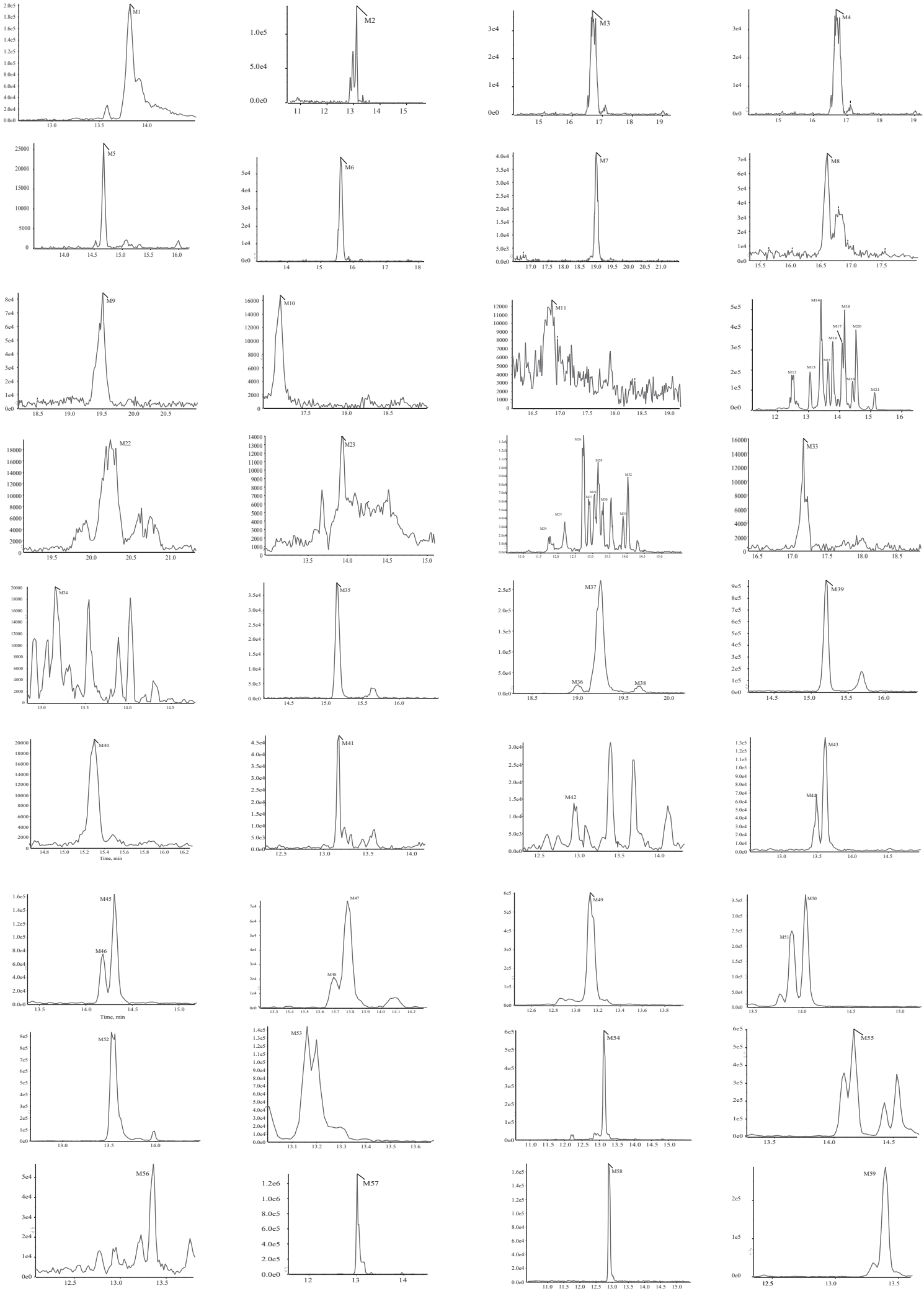

Figure2. XIC of the silybin metabolites in rat tissues and intestinal contents. X-axis is time in minutes Y-axis is response intensity

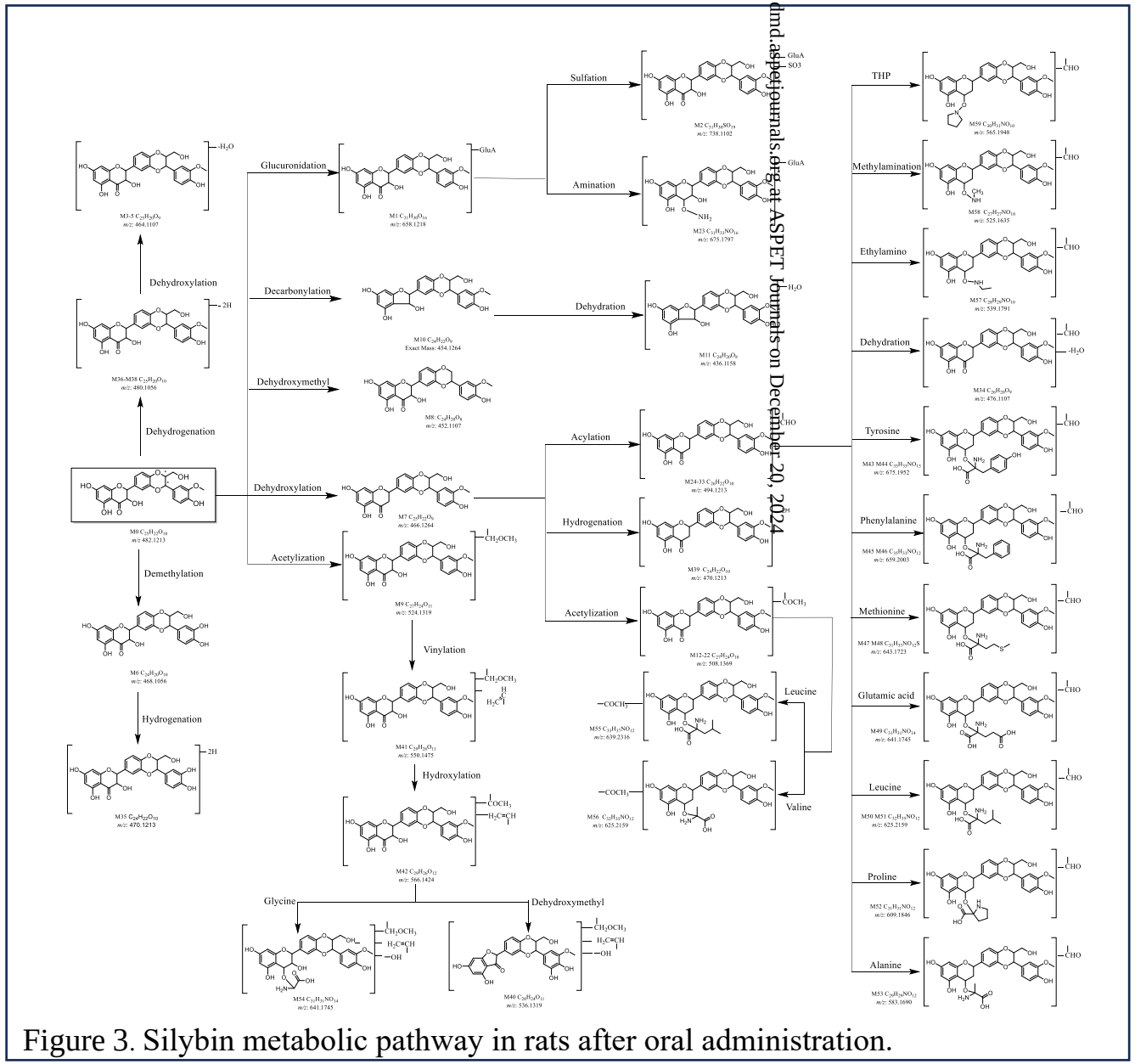

Figure 3. Silybin metabolic pathway in rats after oral administration.

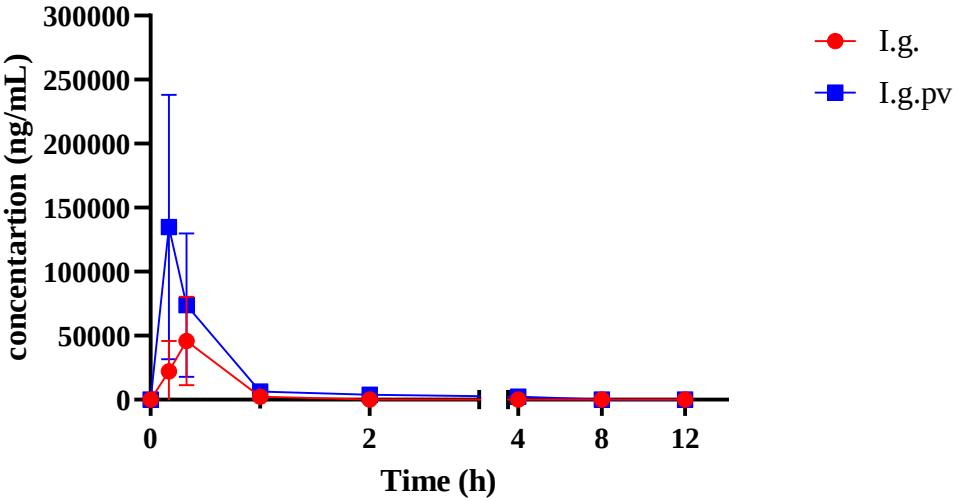

Figure 4. Concentration-time curve of silybin in hepatic vein plasma and abdominal aorta by intragastric administration at 200 mg/kg. (mean ± SD, n = 5). i.g.: intragastric administration; i.g.pv: hepatic portal vein blood collected after intragastric administration

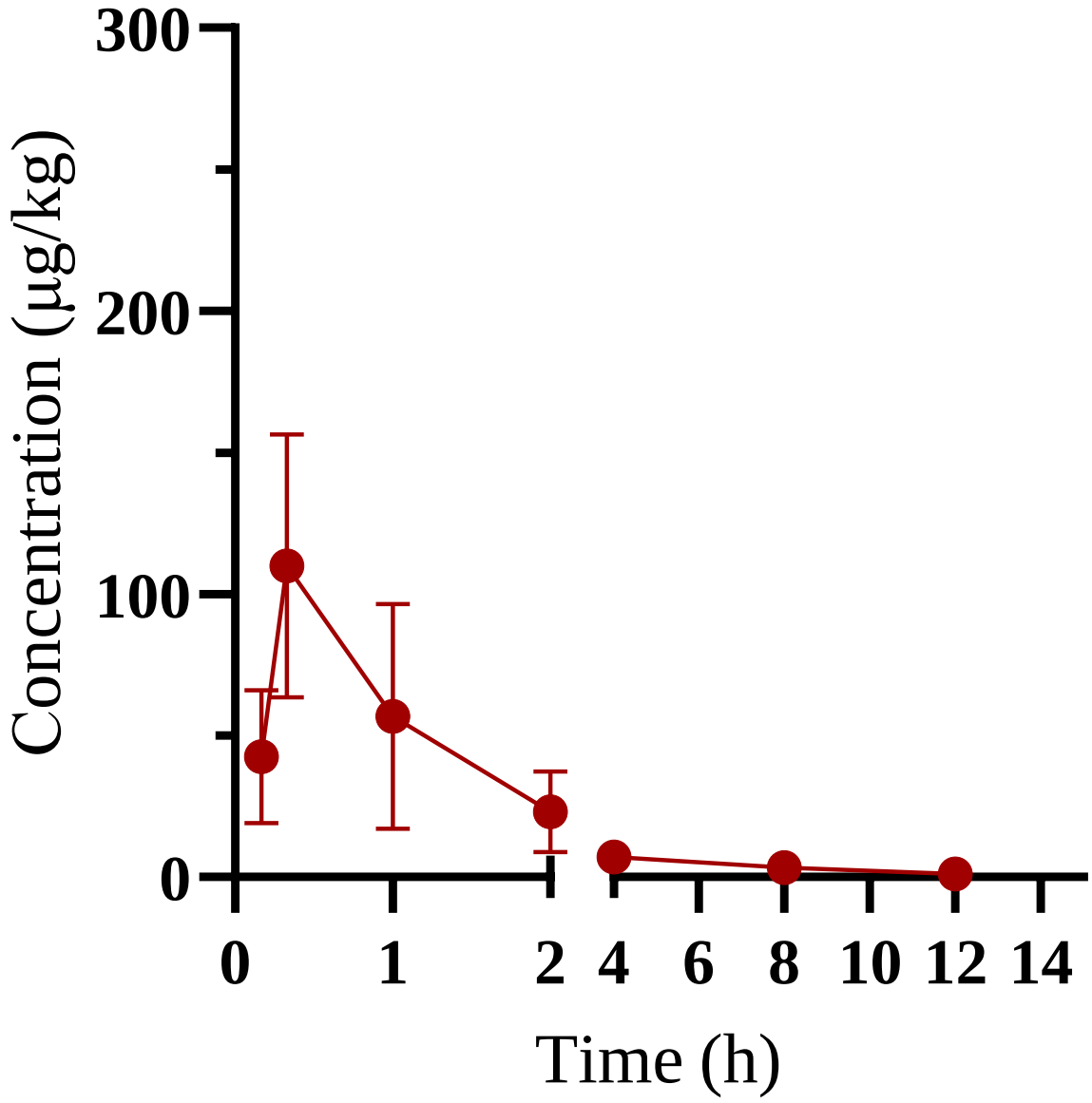

Figure5. Concentration of silybin in the liver by intragastric administration at 200 mg/kg. (mean ± SD, n = 5)